Research Progress of Phase Linking Method in Time-Series InSAR Data Processing

Peng Shen[1,2], Changcheng Wang[3], Mingsheng Liao[4*], Lu Zhang[4], Jie Dong[1], Keren Dai[2]

1 School of Remote Sensing and Information Engineering, Wuhan University; 2 State Key Laboratory of Geohazard Prevention and Geoenvironment Protection, Chengdu University of Technology;
3 School of Geoscience and Info-Physics, Central South University; 4 State Key Laboratory of Information Engineering in Surveying, Mapping and Remote Sensing, Wuhan University

[Project ID. 95358 Geophysical and geodetics retrieval from SAR data stacks over natural scenarios]
[Project ID. 95436 Dynamic deformation monitoring and health diagnosis of infrastructures and surrounding geologic environments with multi-source earth observation data]

1. Introduction

Interferometric Synthetic Aperture Radar (SAR)(InSAR) technology enables the acquisition of wide-area, high-precision surface deformation measurements and is widely applied in geological hazard monitoring. However, its performance is limited by decorrelation problem arising from temporal changes in scatterer characteristics. The Phase Linking (PL) method, which recovers systematic phase series through multi-temporal interferometric phase analysis, has become a core technique for addressing the challenge of monitoring coherence-low surfaces in Time-Series InSAR (TSInSAR) . This report systematically reviews the research motivation, statistical foundation, methodological advancements, result analysis, and future trends of the PL method.

2. Research Motivation

InSAR phase component model is donated as:

$$\phi = \phi_{flat} + \phi_{topo} + \phi_{def} + \phi_{orb} + \phi_{atm} + \phi_{ion} + \phi_{noise} \quad (1)$$

InSAR decorrelation sources are expressed as follows:

$$|\gamma| = |\gamma_{geo}||\gamma_{DC}||\gamma_{proc}||\gamma_{SNR}||\gamma_{temp}||\gamma_{vol}| \quad (2)$$

Due to speckle noise and decorrelation, the phase closure of DS is not equal to 0, i.e.,

$$\neq 0 \phi_{DS}^{m,n,k} = \mathrm{W}\left(\phi^{m,n} + \phi^{n,k} + \phi^{k,m}\right) \neq 0 \quad (3)$$

Hence, to address the phase inconsistency problem, it is necessary to research the PL theory.

3. Statistical Foundation

Acquiring N SAR images, time-series interferometric (*TSIn*) scattering vector is constructed and follows a multivariate complex circular Gaussian distribution (i.e., $\mathrm{P}^{(N,\mathbf{\Sigma}_{TSIn})}(\mathbf{k}_{TSIn})$):

$$\mathbf{k}_{TSIn} = [s^1 \quad \cdots \quad s^N] \quad (4)$$

The *TSIn* coherency matrix is estimated with spatial average of several homogeneous pixels, and can be normalized into the time-series coherence (*TSCoh*) matrix:

$$\mathbf{T}_{TSCoh} = \begin{bmatrix} 1 & |\gamma^{1,2}|\exp(1j\phi^{1,2}) & \cdots & |\gamma^{1,N}|\exp(1j\phi^{1,N}) \\ (|\gamma^{1,2}|\exp(1j\phi^{1,2}))^* & 1 & \cdots & |\gamma^{2,N}|\exp(1j\phi^{2,N}) \\ \vdots & \vdots & \ddots & \vdots \\ (|\gamma^{1,N}|\exp(1j\phi^{1,N}))^* & (|\gamma^{2,N}|\exp(1j\phi^{2,N}))^* & \cdots & 1 \end{bmatrix} \quad (5)$$

The multi-look *TSCoh* matrix follows a complex Wishart distribution (i.e.,$\mathrm{P}^{(N,L,\mathbf{\Sigma}_{TSIn})}(\mathbf{T}_{TSIn})$), whose statistical properties provide a theoretical foundation for the PL parameter estimation.

4. Methodological Advancements

The PL theory utilizes a symmetric coherence magnitude matrix and an interferometric phase matrix to represent the magnitude and phase components of the *TSCoh* matrix, respectively:

$$\mathbf{\Sigma}_{TSCoh} = \mathbf{\Theta}\Upsilon\mathbf{\Theta}^H = \Upsilon \circ \boldsymbol{\theta}\boldsymbol{\theta}^H, \mathbf{\Theta} = \mathrm{diag}(\boldsymbol{\theta}) \quad (6)$$

Based on complex Wishart distribution, the maximum likelihood estimate (MLE) of the phase series $\hat{\boldsymbol{\theta}}$ is derived by maximizing the likelihood function of the matrix sample estimate:

$$\hat{\boldsymbol{\theta}} = \underset{\boldsymbol{\theta}}{\mathrm{argmin}}\{\boldsymbol{\theta}^H(|\mathbf{T}_{TSCoh}|^{-1} \circ \mathbf{T}_{TSCoh})\boldsymbol{\theta}\} \quad (7)$$

The differences among various PL algorithms primarily arise from their weighting strategies and solution approaches, as shown in Tab. 1.

Tab. 1 Classification and Comparison of Mainstream PL Methods.

Method Category	Baseline Network	Classical Algorithm	Weighting Strategies	Regularization Method	Feature
Optimization Estimation	Full Intf Combination	PTA、TMLE	MLE	Common Regularization, etc.	1. Depends on the initial value and number of iterations 2. Low computing efficiency
	Full Intf Combination	ILS、NLE	Fisher Information	—	
	Block-Based Full Intf Combination	SE	MLE	Common Regularization	
	Small BaselineSet	StBAS	MLE	Common Regularization	
Eigenvalue Decomposition	Full Intf Combination	PCA	Coherence Weighting	—	1. Multiple scattering mechanisms can be separated. 2. Computational efficiency depends on the number of decomposition times.
	Full Interf Combination	EMI	MLE	Common Regularization	
	Full Intf Combination	EPL	Temporal Decorrelation Model-Based MLE	Common Regularization	
	Small BaselineSet	AdpPL	MLE	Adaptive Regularization	

6. Future Trends

- The PL methods have made significant progress in improving phase accuracy and algorithm efficiency, but they still face several challenges, including the low efficiency of regularized solutions and interference from physical factors like soil moisture.
- As spaceborne SAR satellites advance toward multi-band, multi-polarization, and high spatio-temporal resolution, the application of PL methods in multi-band data fusion, non-Gaussian characteristics of high-resolution imagery, and monitoring in vegetated areas will encounter new technical difficulties.

5. Simulated and Real Experimental Results and Analyses

- The simulated experiment uses the Monte Carlo simulation to generate the multilooking time-series covariance matrix under both exponential and seasonal temporal decorrelation models, and quantificationally compare five classical PL methods, including PTA, PCA, EMI, StBAS, and AdpPL, in terms of interferometric phase optimization, deformation measurement accuracy and algorithm computational efficiency.
- In the real experiment, the Daguangbao landslide triggered by the “5.12” Wenchuan Mw 7.9 earthquake and the 56 scenes of Senetinel-1 SAR images in VV polarization are selected as the experimental data and the study area, respectively. In addition to the persistent scatterer interferometric (PSI) technology, three PL methods, including PTA, EMI, and AdpPL are qualitatively compared and analyzed in the three aspects, similar to the simulated experiment.

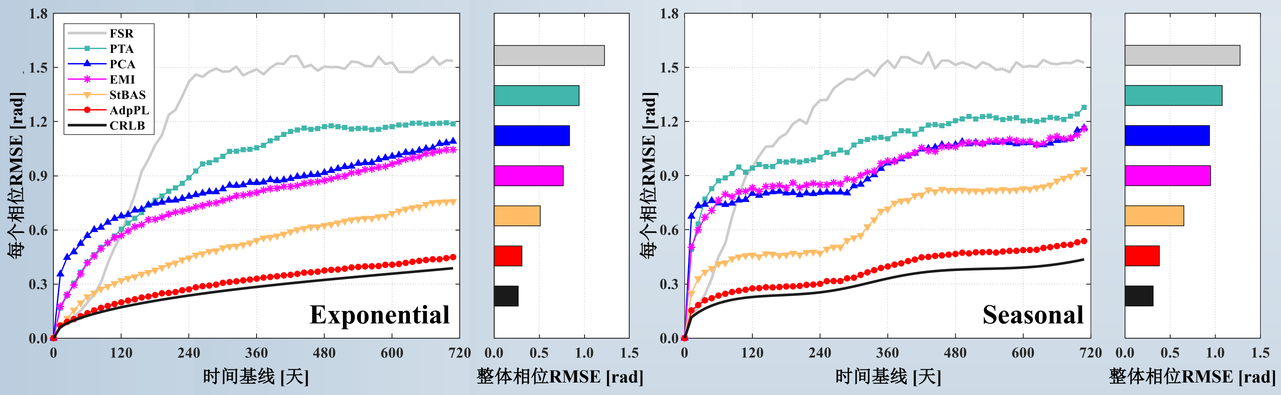


Fig. 1 ESR Phase RMSE of Different PL Methods under Two Temporal Decorrelation Models.

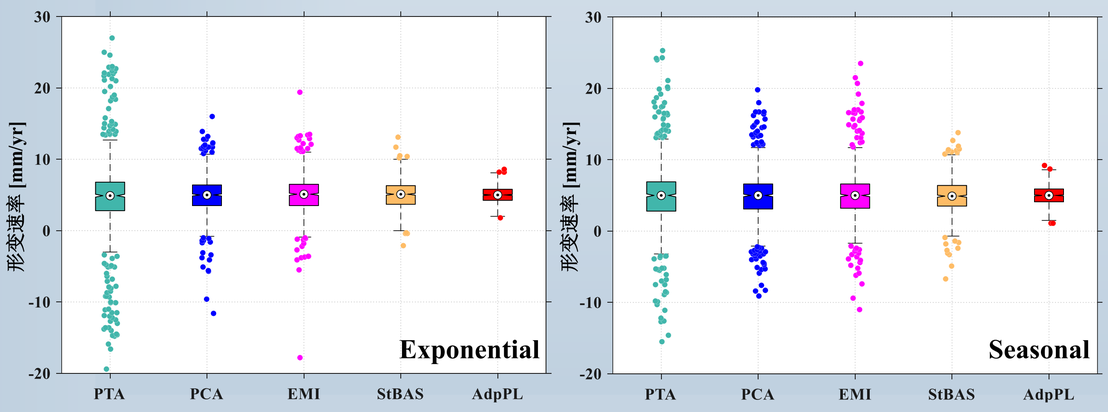


Fig. 2 Rate Boxplot of Different PL Methods under Two Temporal Decorrelation Models.

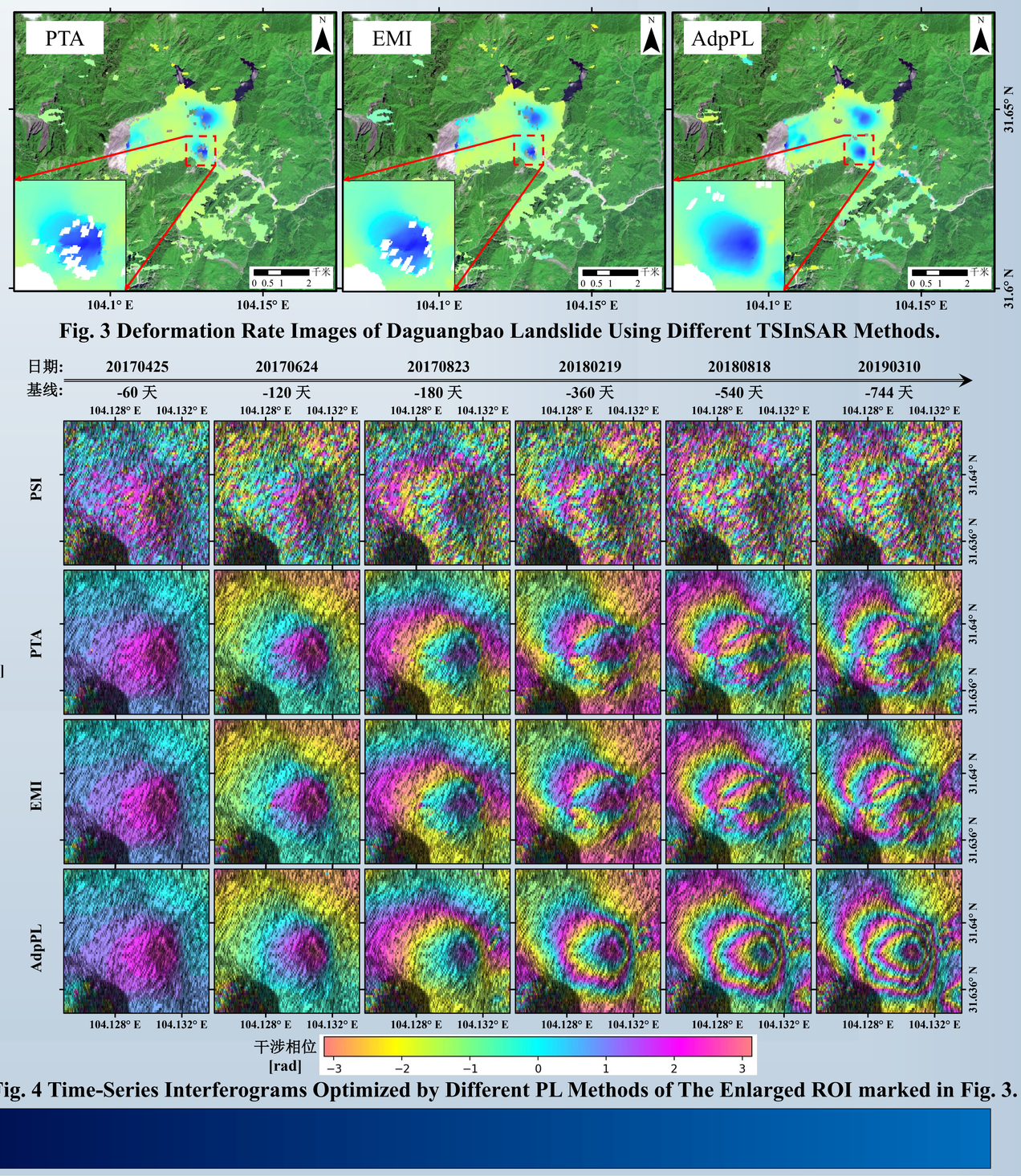


Fig. 3 Deformation Rate Images of Daguangbao Landslide Using Different TSInSAR Methods.

Fig. 4 Time-Series Interferograms Optimized by Different PL Methods of The Enlarged ROI marked in Fig. 3.

Contact

Email: shen-peng@whu.edu.cn

The data and code related to the experiments have been uploaded to GitHub: https://github.com/shen-pengsar.